

Mesophase Structure of Low-Wetting Liquid Crystalline Polyacrylates with New Perfluoroalkyl Benzoate Side Groups

ELISA MARTINELLI,¹ FRANCESCA PAOLI,¹ BERNARD GALLOT,² GIANCARLO GALLI¹

¹Dipartimento di Chimica e Chimica Industriale, Udr Pisa INSTM, Università di Pisa, via Risorgimento 35, Pisa 56126, Italy

²Laboratoire des Matériaux Organiques à Propriétés Spécifiques, CNRS, Vernaison 69390, France

Received 30 April 2010; accepted 28 June 2010

DOI: 10.1002/pola.24207

Published online in Wiley Online Library (wileyonlinelibrary.com).

ABSTRACT: The synthesis, thermal behavior, bulk microstructure, and wettability of new polyacrylates carrying spaced 4-perfluorohexylpropyl benzoate and 4-perfluorooctylpropyl benzoate units in the side groups were investigated. X-ray diffraction analysis proved the formation of different smectic mesophases (SmI₂, SmF₂, and SmC₂) and the evolution of their structures and lattice parameters with temperature. The mesophase polymorphic behavior depended on the length of the perfluorinated chain segment in the repeat unit. The electron density profiles along the smectic layer normal were drawn and provided a deeper insight into the packing of the side

chains in a tilted, double layer structure. Thin polymer films were cast from solution, and their low wettability was established by measurements of contact angles with different probing liquids. We suggest that the hydrophobicity and lipophobicity of the films are enhanced by the mesophase surface structure which is mediated by the high-order, mesophase bulk structure. © 2010 Wiley Periodicals, Inc. *J Polym Sci Part A: Polym Chem* 48: 4128–4139, 2010

KEYWORDS: fluoropolymers; liquid-crystalline polymers; mesophase structure; surface energy; thin films; wettability

INTRODUCTION Fluorinated liquid crystalline polymers are a relatively new class of fluoropolymers; see illustrations of different structural classes of polymers.^{1–9} Initial studies on fluorinated liquid crystals focused on partly fluorinated alkanes, namely diblock hydrocarbon-fluorocarbon molecules such as H(CH₂)_x(CF₂)_yF ($x, y > \sim 6$).^{10–14} The ability of these compounds was shown to form thermotropic mesophases because of the strong intramolecular phase segregation¹⁵ and the rigid, rod-like nature of the fluorocarbon chains.^{16,17} Moreover, the tendency to aggregation of amphiphilic, fluorinated molecules in solutions also manifested in the formation of different lyotropic mesophases.^{18,19} Later synthetic efforts resulted in the development of a diversity of liquid crystalline materials, including low molar mass compounds,²⁰ polymers,^{1,5,21–25} and supramolecular structures^{26–28} in which the length of the fluorinated mesogen $-(CH_2)_x(CF_2)_yF$ was varied in a range of numbers x and y , most common examples having $x = 2, y > 6$. More conventional mesogenic units, for example, biphenyls and bisbenzoates, have also been used in combination with partly fluorinated tails in low molar mass^{29–33} and polymeric liquid crystals.^{6,25}

Such fluorinated polymers have lately been considered as candidate materials for the macromolecular engineering of low-surface energy films through self-organization. In fact, spontaneous assembling over different length scales may be driven

by several mechanisms, including liquid crystallinity and surface segregation.³⁴ Under some circumstances, these mechanisms may be used together to form an ordered surface structure. For instance, block copolymers phase separate to preferred microstructures, but when low-surface energy blocks are incorporated, surface and interface segregation will also take place to create further organization in the region of the low energy surface.^{4,5,35,36} In particular, liquid crystallinity may provide a useful means for preparing low-surface energy polymeric materials for nonstick coating application.^{9,23,37} The attachment of a fluorinated mesogen pendent to a polymer backbone can further improve and stabilize the surface structure and order, for example, upon exposure to different polar environments, as a consequence of the induced mesomorphic behavior in the bulk of the material.

In this study, we designed and prepared new polyacrylates, p(**1-6**) and p(**1-8**), carrying a perfluoroalkylpropyl benzoate side group that was spaced from the polymer backbone and had a varied length of the perfluorocarbon chain segment (6 and 8 CF₂ groups, respectively). The new molecular architecture was preferred to those of the largely used perfluoroalkylethyl mesogens because it was expected to enhance the mesogenic tendency of the polymers and to promote formation of a mesophase organized over different scales from the molecular level upwards. This was connected with a pronounced hydrophobic and lipophobic behavior of the polymer

Correspondence to: G. Galli (E-mail: gallig@cci.unipi.it)

Journal of Polymer Science: Part A: Polymer Chemistry, Vol. 48, 4128–4139 (2010) © 2010 Wiley Periodicals, Inc.

films, with the longer perfluorocarbon chain determining a lower wettability. An interplay between bulk structure and surface properties is discussed.

EXPERIMENTAL

Starting Materials

The solvents were dried and distilled by conventional methods and then handled under anhydrous nitrogen atmosphere. α,α' -Azo-bis(isobutyronitrile) (AIBN) was recrystallized from methanol. Acrylic acid was distilled under reduced nitrogen pressure. Acryloyl chloride was distilled under nitrogen. 4-Hydroxybenzoic acid (**3**), ethyl 4-hydroxybenzoate (**7**), 4-pyrrolidinopyridine (PPy), *N,N'*-dicyclohexylcarbodiimide (DCC), allyl bromide, allyl alcohol, perfluorohexyl iodide, perfluorooctyl iodide, and 9-borabicyclononane (9-BBN) (0.5 M solution in tetrahydrofuran) were purchased from Aldrich and used without further purification.

Synthesis of Monomers

4-(2-Propenyl-1-oxy)benzoic acid (**4**)

29.88 g (0.22 mol) of (**3**), 26.55 (0.47 mol) of KOH, and 2.96 g (0.018 mol) of KI were dissolved in 750 mL of 80% ethanol. 26.56 g (0.21 mol) of allyl bromide was slowly added to the solution, and the resulting mixture was refluxed for 3 days. The solvent was evaporated under vacuum, and the solid residue was dissolved in water. The mixture was acidified to pH \sim 1, and the solid precipitated was filtered off and thoroughly washed with water. The crude product was purified by crystallization from methanol, giving pure (**4**) (m.p. 164–165 °C) in 58% yield.

$^1\text{H-NMR}$ (DMSO- d_6) δ (ppm) = 12.6 (1H, COOH), 7.9 (2H, aromatic), 7.0 (2H, aromatic), 6.0 (1H, $\text{CH}_2=\text{CH}$), 5.3 (2H, $\text{CH}_2=\text{CH}$), 4.6 (2H, CH_2OPh).

FTIR (KBr pellet) (cm^{-1}) = 3300–2500 (ν O—H), 1685 (ν C=O), 1560 (ν C=C aromatic), 1429 and 1320 (δ C—H vinyl), 999 and 949 (ν C—H vinyl).

3-(Perfluorohexyl)-1-propanol (**2-6**)

0.13 g (0.8 mmol) of AIBN was added incrementally over a period of 45 min to a solution of 24.44 g (54.0 mmol) of perfluorohexyl iodide and 4.77 g (82.0 mmol) of allyl alcohol at 80 °C under nitrogen atmosphere. The reaction was then carried out at 80 °C for another 5 h. The volatile compounds were removed under vacuum, and the resulting 2-iodo-3-(perfluorohexyl)-1-propanol was dissolved in 125 mL of anhydrous diethyl ether. The solution was added dropwise to 50 mL (50.0 mmol) of 1 M solution of LiAlH_4 in diethyl ether under nitrogen atmosphere. The reaction mixture was kept at room temperature overnight and then hydrolyzed with 9 mL of water, 11 mL of 10% NaOH, and finally 9 mL of water. After filtration of the precipitate, the solvent was evaporated under vacuum. The crude product was purified by column chromatography (silica gel, eluent *n*-hexane/ethyl acetate 3:2 v/v), giving (**2-6**) as a pale yellow liquid in 49% yield.

$^1\text{H-NMR}$ (CDCl_3) δ (ppm) = 3.8 (2H, CH_2OH), 2.3 (2H, CH_2CF_2), 1.9 (2H, $\text{CH}_2\text{CH}_2\text{OH}$), 1.7 (1H, CH_2OH).

FTIR (film) (cm^{-1}) = 3330 (ν O—H), 2958–2888 (ν C—H aliphatic), 1146 (ν C—F), 654 (ω CF_2).

3-(Perfluorohexyl)-1-propyl 4-(2-propenyl-1-oxy)benzoate (**5**)

1.70 g (9.5 mmol) of (**4**), 3.60 g (9.5 mmol) of (**2-6**) and 0.15 g (0.9 mmol) of PPy were dissolved in 60 mL of anhydrous dichloromethane under nitrogen atmosphere. A solution of 1.97 g (9.5 mmol) of DCC in 30 mL of the same solvent was slowly dropped at 0 °C. The reaction was carried out under stirring at room temperature for 3 days. The solid precipitated was filtered off, and the organic phase was washed with 5% HCl, 5% NaHCO_3 and water to neutrality. The organic phase was dried over anhydrous Na_2SO_4 , and the solvent was then evaporated under vacuum. The crude product was purified by column chromatography (silica gel, eluent *n*-hexane/ethyl acetate 3:2 v/v) to give pure (**5**) in 51% yield as a pale yellow liquid.

$^1\text{H-NMR}$ (CDCl_3) δ (ppm) = 8.0 (2H, aromatic), 7.0 (2H aromatic), 6.1 (1H, $\text{CH}_2=\text{CH}$), 5.4 (2H, $\text{CH}_2=\text{CH}$), 4.6 (2H, COOCH_2), 4.4 (2H, CH_2OPh), 2.3–2.1 (4H, $\text{CH}_2\text{CH}_2\text{CF}_2$).

FTIR (KBr film) (cm^{-1}) = 3100–3050 (ν C—H vinyl and aromatic), 1716 (ν C=O), 1144 (ν C—F), 654 (ω CF_2).

3-(Perfluorohexyl)-1-propyl 4-(3-hydroxypropyl-1-oxy)benzoate (**6**)

2.00 g (3.7 mmol) of (**5**) in 2 mL of tetrahydrofuran was added dropwise to 7.4 mL (3.7 mmol) of a 0.5-M solution of 9-BBN in tetrahydrofuran under nitrogen at reflux. The reaction was carried out at reflux for 4 h. The crude intermediate organoborane was oxidized by adding simultaneously 1.5 mL (49.0 mmol) of 30% H_2O_2 and 0.8 mL (4.8 mmol) of a 6-M solution of sodium acetate at 0 °C. The reaction mixture was kept under stirring at room temperature overnight. The aqueous phase was saturated with NaCl and K_2CO_3 and then extracted with tetrahydrofuran. The organic phase was washed with water and then dried over Na_2SO_4 . The solvent was evaporated under vacuum, and the crude product was purified by column chromatography (silica gel, eluent *n*-hexane/ethyl acetate 1:1 v/v). The white solid was further purified by crystallization from *n*-hexane to give pure (**6**) in 69% yield (m.p. 48–50 °C).

$^1\text{H-NMR}$ (CDCl_3) δ (ppm) = 7.9 (2H, aromatic), 6.9 (2H, aromatic), 4.4 (2H, COOCH_2), 4.2 (2H, CH_2OPh), 3.8 (2H, CH_2OH), 2.4–2.0 (6H, $\text{CH}_2\text{CH}_2\text{CF}_2$, $\text{CH}_2\text{CH}_2\text{OH}$), 1.8 (1H, CH_2OH).

FTIR (KBr pellet) (cm^{-1}) = 3500–3300 (ν O—H), 3100–3000 (ν C—H aromatic), 1714 (ν C=O), 1144 (ν C—F), 654 (ω CF_2).

3-(Perfluorohexyl)-1-propyl 4-(3-acryloyloxypropyl-1-oxy)benzoate (**1-6**)

A solution of 0.45 g (2.0 mmol) of DCC in 5 mL of anhydrous dichloromethane was slowly dropped to a solution of 1.11 g (2.0 mmol) of (**6**), 0.14 mL (2.0 mmol) of acrylic acid and 0.03 g (0.2 mmol) of PPy in 10 mL of CH_2Cl_2 under nitrogen at 0 °C. The reaction was carried out at room temperature for 4 days. The solid precipitated was filtered off, and the organic phase was washed with 5% HCl, 5% NaHCO_3 and water and dried over anhydrous Na_2SO_4 . The solvent was

then evaporated under vacuum, and the crude product was purified by column chromatography (silica gel, eluent *n*-hexane/ethyl acetate 2:1 v/v) to give pure (**1–6**) as a pale yellow solid (m.p. 34–36 °C) in 35% yield.

$^1\text{H-NMR}$ (CDCl_3) δ (ppm) = 8.0 (2H, aromatic), 6.9 (2H, aromatic), 6.5 (1H, CH=), 6.2 (1H, CH=), 5.8 (1H, CH=), 4.4 (4H, PhCOOCH_2 , CH_2OPh), 4.2 (2H, $\text{CH}_2=\text{CHCOOCH}_2$), 2.2 (6H, $\text{CH}_2\text{CH}_2\text{CF}_2$, $\text{CH}_2\text{CH}_2\text{OPh}$).

FTIR (KBr pellet) (cm^{-1}) = 3100–3050 (ν C–H vinyl and aromatic), 1718 and 1706 (ν C=O), 1142–1122 (ν C–F), 656 (ω CF_2).

$^{19}\text{F-NMR}$ ($\text{CDCl}_3/\text{CF}_3\text{COOH}$) δ (ppm) = –5 (3F, CF_3), –38 (2F, CH_2CF_2), –46 to –48 (6F, CF_2), –51 (2F, CF_2CF_3).

4-(3-Hydroxypropyl-1-oxy)benzoic Acid (**9**)

In a first step, 8.7 g (52.0 mmol) of (**7**) and 8.2 g (78.0 mmol) K_2CO_3 were dissolved in 100 mL of anhydrous 2-butanone and a solution of 8.0 g (57.0 mmol) of 1-bromo-3-propanol in 8.0 mL of anhydrous 2-butanone was slowly added at reflux. The reaction mixture was kept at reflux for 48 h and then cooled down to room temperature and filtered. The solvent was removed under vacuum, and the crude product was crystallized from methanol to give pure ethyl 4-(3-hydroxypropyl-1-oxy)benzoate (**8**) in 98% yield.

In a second step, 11.5 g (51.0 mmol) of (**8**) was added to a solution of 4.25 g (75.0 mmol) KOH in 175 mL of ethanol and 125 mL of water. The reaction was carried out at reflux for 6 h. The mixture was acidified with 37% HCl to pH \sim 2 and extracted with CH_2Cl_2 . The organic phase was dried over Na_2SO_4 , and the solvent was evaporated under vacuum. The crude product was purified by crystallization from methanol to give pure (**9**) as a white solid in 97% yield.

$^1\text{H-NMR}$ (CDCl_3) δ (ppm) = 7.9 (2H, aromatic), 7.0 (2H, aromatic), 4.1 (2H, CH_2OPh), 3.5 (2H, CH_2OH), 1.8 (2H, $\text{CH}_2\text{CH}_2\text{OH}$).

4-(3-Acryloyloxypropyl-1-oxy)benzoic Acid (**10**)

5.50 g (28.0 mmol) of (**9**), 5.68 g (56.0 mmol) of triethylamine and 5 mg of 2,6-dit-butyl-4-cresol were dissolved in 150 mL of anhydrous tetrahydrofuran. 3.30 g (37.0 mmol) of acryloyl chloride was added dropwise to the solution at 0 °C under vigorous stirring. The reaction mixture was kept at room temperature for 16 h and at 45 °C for 3 h. The solvent was removed under vacuum, and the solid residue was dissolved in CHCl_3 and washed with 5% HCl and water. The organic phase was dried over Na_2SO_4 overnight. The solvent was removed under vacuum and the crude product was purified by column chromatography (silica gel, eluent *n*-hexane/ethyl acetate 1:1 v/v) to give pure (**10**) as a white solid (m.p. 122–124 °C) in 30% yield.

$^1\text{H-NMR}$ (CDCl_3) δ (ppm) = 8.0 (2H, aromatic), 6.9 (2H, aromatic), 6.4 (1H, CH=), 6.1 (1H, CH=), 5.8 (1H, CH=), 4.4 (2H, COOCH_2), 4.1 (2H, CH_2OPh), 2.2 (2H, $\text{CH}_2\text{CH}_2\text{OPh}$).

3-(Perfluorooctyl)-1-propanol (**2–8**)

0.06 g (0.4 mmol) of AIBN was added incrementally over a period of 45 min to a solution of 13.64 g (25.0 mmol) of perfluorooctyl iodide and 2.17 g (37.5 mmol) of allyl alcohol

under nitrogen atmosphere at 80 °C. The reaction mixture was kept under stirring at 80 °C for another 5 h. The volatile compounds were removed under vacuum, and the resulting 2-iodo-3-(perfluorooctyl)-1-propanol was dissolved in 125 mL of anhydrous diethyl ether. The solution was added dropwise to a 50 mL (50.0 mmol) of 1 M solution of LiAlH_4 in the same solvent under nitrogen atmosphere. The reaction mixture was kept at room temperature overnight and then hydrolyzed with 4 mL of water, 5 mL of 10% NaOH, and finally 4 mL of water. The precipitate was filtered off, and the solvent was evaporated under vacuum. The crude product was purified by sublimation under high vacuum giving pure (**2–8**) as a white solid (m.p. 43–45 °C) in 45% yield.

$^1\text{H-NMR}$ (CDCl_3) δ (ppm) = 3.8 (2H, CH_2OH), 2.3 (2H, CH_2CF_2), 1.9 (2H, $\text{CH}_2\text{CH}_2\text{OH}$), 1.5 (1H, CH_2OH).

FTIR (film) (cm^{-1}) = 3244 (ν O–H), 1150 (ν C–F), 658 (ω CF_2).

3-(Perfluorooctyl)-1-propyl 4-(3-acryloyloxypropyl-1-oxy)benzoate (**1–8**)

A solution of 0.61 g (3.0 mmol) of DCC in 15 mL of anhydrous CH_2Cl_2 was added dropwise to a solution of 1.42 g (3.0 mmol) of (**2–8**), 0.75 g (3.0 mmol) of (**10**), 0.04 g (0.3 mmol) of PPy in 25 mL of anhydrous CH_2Cl_2 under nitrogen atmosphere at 0 °C. The solution at 0 °C under vigorous stirring. The reaction was carried out at room temperature for 3 days. The precipitate formed was filtered off, and the organic phase was washed with 5% HCl, 5% NaHCO_3 and water, and dried over Na_2SO_4 . The solvent was then evaporated under vacuum, and the crude product was purified by column chromatography (silica gel, eluent *n*-hexane/ethyl acetate 3:1 v/v) to give pure (**1–8**) as a white solid (m. p. 42–45 °C) in 45% yield.

$^1\text{H-NMR}$ (CDCl_3) δ (ppm) = 8.0 (2H, aromatic), 6.9 (2H, aromatic), 6.5 (1H, CH=), 6.1 (1H, CH=), 5.8 (1H, CH=), 4.4 (4H, PhCOOCH_2 , CH_2OPh), 4.1 (2H, $\text{CH}_2=\text{CHOOCH}_2$), 2.2 (6H, $\text{CH}_2\text{CH}_2\text{CF}_2$, $\text{CH}_2\text{CH}_2\text{OPh}$).

FTIR (KBr pellet) (cm^{-1}) = 3076 (ν C–H vinyl and aromatic), 1712 and 1711 (ν C=O), 1172 (ν C–F), 652 (ω CF_2).

$^{19}\text{F-NMR}$ ($\text{CDCl}_3/\text{CF}_3\text{COOH}$) δ (ppm) = –6 (3F, CF_3), –38 (2F, CH_2CF_2), –46 to –49 (10F, CF_2), –51 (2F, CF_2CF_3).

Synthesis of Polymers

p(**1–6**)

0.29 g (0.48 mmol) of monomer (**1–6**), 3 mg of AIBN and 3 mL of anhydrous benzene were introduced into a Pyrex vial and degassed by several freeze-thaw pump cycles. The polymerization was carried out at 60 °C for 48 h. The polymer was purified by several precipitations into methanol from chloroform/1,1,2-trichlorotrifluoroethane solutions giving a powdery white polymer in 70% yield.

$^1\text{H-NMR}$ (CDCl_3) δ (ppm) = 7.9 (2H, aromatic), 6.8 (2H, aromatic), 4.3 (4H, COOCH_2), 4.0 (2H, CH_2OPh), 2.2 (6H, $\text{CH}_2\text{CH}_2\text{CF}_2$, $\text{CH}_2\text{CH}_2\text{OPh}$), 1.7–1.2 (3H, CH_2CH).

^{19}F -NMR ($\text{CDCl}_3/\text{CCl}_2\text{FCClF}_2/\text{CF}_3\text{COOH}$) δ (ppm) = -14 (3F, CF_3), -47 (2F, CF_2CH_2), -54 to -56 (6F, CF_2), -59 (2F, CF_2CF_3).

FTIR (KBr pellet) (cm^{-1}) = 3100 – 3050 (ν C–H aromatic), 2962 – 2850 (ν C–H aliphatic), 1714 and 1712 (ν C=O), 1144 (ν C–F), 652 (ω CF_2).

***p*(1–8)**

0.50 g (0.7 mmol) of monomer (1–8), 6 mg of AIBN and 3 mL of anhydrous benzene were introduced into a Pyrex vial and degassed by several freeze-thaw pump cycles. The polymerization was carried out at 60 °C for 48 h. The polymer was purified by several precipitations into methanol from chloroform/1,1,2-trichlorotrifluoroethane solutions giving a powdery white polymer in 85% yield.

^1H -NMR (CDCl_3) δ (ppm) = 7.9 (2H, aromatic), 6.8 (2H, aromatic), 4.3 (4H, COOCH_2), 3.9 (2H, CH_2OPh), 2.1 (6H, $\text{CH}_2\text{CH}_2\text{CF}_2$, $\text{CH}_2\text{CH}_2\text{OPh}$), 1.6 – 1.2 (3H, CH_2CH).

^{19}F -NMR ($\text{CDCl}_3/\text{CCl}_2\text{FCClF}_2/\text{CF}_3\text{COOH}$) δ (ppm) = -14 (3F, CF_3), -47 (2F, CF_2CH_2), -54 to -56 (10F, CF_2), -59 (2F, CF_2CF_3).

FTIR (KBr pellet) (cm^{-1}) = 3080 – 3050 (ν C–H aromatic), 2962 – 2860 (ν C(H aliphatic), 1714 and 1712 (ν C=O), 1150 (ν C–F), 658 (ω CF_2).

Polymer Films

The polymer films were prepared by casting a 5 wt % solution of the polymer in trifluorotoluene or 1,1,2-trichlorotrifluoroethane on glass cover-slips and letting the solvent to evaporate slowly at room temperature. The films were annealed at 10 °C below the isotropization temperature of the polymer for 48 h and then slowly cooled to room temperature before the measurements (thickness 100 – 150 μm).

Characterization

^1H and ^{13}C spectra were recorded on Varian Gemini VRX 200. ^{19}F spectra were recorded on Varian Gemini VRX 300.

Light scattering measurements were performed with a He–Ne laser source ($\lambda = 633$ nm) using a Sofica 4200 photogoniometer. The refractive index increments were also measured with a KMX 16 laser differential refractometer at the same wavelength.

Differential scanning calorimetry (DSC) measurements were performed with a Mettler DSC-30 instrument (10 °C/min scanning rate). The clearing or isotropization transition temperature (T_i) was taken at the maximum temperature in the DSC enthalpic peak of the second heating cycle. The glass transition temperature (T_g) was set at the half-devitrification temperature.

Polarizing optical microscopy observations were performed on polymer powder sandwiched between glass slides. A Reichert-Jung Polyvar microscope equipped with a programmable Mettler FP52 heating stage was used. The birefringent melts were analyzed on heating up to and on cooling from T_i at a scanning rate of 3 – 10 °C/min.

Wide-angle X-ray diffraction (WAXD) patterns were recorded with a home-made diffractometer equipped with a flat film

camera. The Ni-filtered $\text{CuK}\alpha$ radiation was used ($\lambda = 1.54$ Å). Polymer powder samples were studied from room temperature up to the temperature of disappearance of the low-angle first-order diffraction signal. The length l_1 of the mesogenic side chain group and the thickness l_2 of the polymer main chain were calculated from the known bond angles and lengths, assuming the repeat unit to be in its fully extended conformation with the fluorocarbon segment in a twisted zigzag conformation of span $p = 2.59$ Å.³⁸ The length $L = 2l_1 + l_2$ for the repeat unit with two side chain groups pointing to opposite directions of the polymer chain was used to evaluate a maximum tilt angle ϕ in the smectic mesophases with an experimental interlayer spacing d ($d = L\cos\phi$).

Several exposures were taken so as to measure the strongest and the weakest reflections. Experimental amplitudes, a_m , of diffraction for the different orders of reflection from the smectic layers were corrected for the Lorentz-polarization factor.

Taking into account the centrosymmetry of the mesophase structure, the electron density profile $\rho(z)$ along the layer normal was given by eq 1³⁹:

$$\rho(z) = \sum_{m=1} [a_m \cos(m2\pi z/d)] \quad (1)$$

where a_m is the amplitude of m th reflection. Being not possible to measure the absolute intensity and amplitude of the different reflection orders, a_m were obtained by normalizing the intensity of each order to the respective first order reflection. The signs of the coefficients a_m were also unknown; it was therefore possible to combine them in 2^m permutations leading to 2^m different electron density profiles.⁴⁰

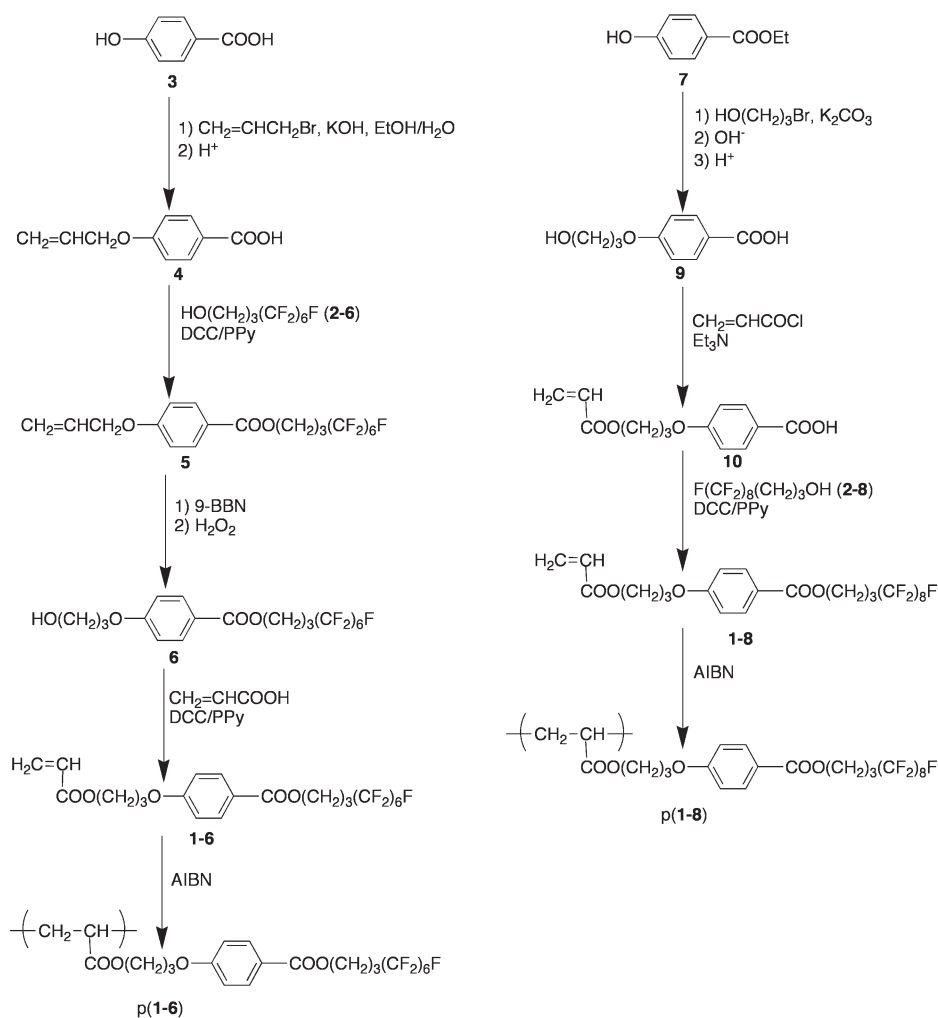
Tapping-mode atomic force microscopy (TM-AFM) measurements were performed by imaging samples with a Digital Instruments Nanoscope IIIa with a Multimode Head. Topographic and phase contrast imaging experiments were performed on 1×1 μm^2 regions. Nanoprobe cantilevers (225 μm , Digital Instrument) were utilized. Phase contrast AFM was carried out at set-point amplitude to cantilever free-oscillation amplitude (A_{sp}/A_0) ratios higher than 0.8 , which is generally regarded as low tapping force. The root-mean-square roughness (RMS) was calculated by the software as $(\sum_i Z_i^2/N)^{0.5}$, where Z_i is the height value and N the number of points measured on the surface analyzed.

Contact angles θ were measured with a Ramè-Hart 230 goniometer using 4 μL drops of water and n -alkanes (heptane, octane, decane, dodecane, and hexadecane) as interrogating liquids (purity > 99%). The values of θ were used to evaluate the solid surface tension γ_s of the polymer films following two different methods.

In the additive component method of Owens and Wendt⁴¹ and Kaelble⁴² the solid surface tension

$$\gamma_s = \gamma_s^d + \gamma_s^p \quad (2)$$

combined with the Young's equation yields



SCHEME 1 Routes for the synthesis of the acrylic monomers and the respective polymers.

$$\gamma_L(1 + \cos \theta) = 2 \left[(\gamma_S^d \gamma_L^d)^{1/2} + (\gamma_S^p \gamma_L^p)^{1/2} \right] \quad (3)$$

where γ^d and γ^p are the dispersion and the polar components, respectively, of the solid, γ_S , and liquid, γ_L , surface tensions; vapor adsorption is assumed to be negligible. By measuring the contact angles of at least two liquids, one polar and one nonpolar, on the same surface two equations can be obtained from which the two unknowns (γ_S^d and γ_S^p) of the solid can be calculated. The total surface energy of the polymer is computed as the sum of the γ_S^d and γ_S^p terms.

The equation-of-state method of Li and Neumann⁴³ involves:

$$\cos \theta = -1 + 2(\gamma_S/\gamma_{LV})^{1/2} \exp[-\beta(\gamma_{LV} - \gamma_S)^2] \quad (4)$$

by which, for a given set of liquid surface tensions γ_{LV} and θ measured on one and the same solid surface, the constant β and solid surface tension γ_S values can be determined by a least-square analysis technique.

RESULTS AND DISCUSSION

Synthesis

The novel acrylic monomers (**1-6**) and (**1-8**) differed for the length of the fluorocarbon chain in the 3-(perfluoroalkyl)-

propyl segment, 6 and 8 CF_2 groups, respectively. The synthesis of the two monomers was carried out following two different routes from easily available, commercial products (Scheme 1).

Monomer (**1-6**) was prepared in four steps. In a first step, 4-hydroxybenzoic acid (**3**) was reacted with allyl bromide. The resulting 4-substituted benzoic acid (**4**) was reacted with 3-(perfluorohexyl)-1-propanol (**2-6**) to yield the respective benzoate ester (**5**) using dicyclohexylcarbodiimide (DCC) as a condensing agent and 4-pyrrolidinopyridine (PPy) as a nucleophilic activator. Then (**5**) was reacted with 9-borabicyclononane (9-BBN) and the intermediate organoborane was oxidized with alkaline hydrogen peroxide to give the corresponding alcohol (**6**). In a fourth step, (**6**) was converted to the desired 3-(perfluorohexyl)-1-propyl 4-(3-acryloyloxypropyl-1-oxy)benzoate (**1-6**) monomer by esterification reaction with acrylic acid in the presence of DCC and PPy.

Monomer (**1-8**) was prepared in three steps. In a first step, ethyl 4-hydroxybenzoate (**7**) was etherified with 3-bromopropan-1-ol under Williamson reaction conditions, and the 4-substituted benzoate intermediate was hydrolyzed to give the corresponding benzoic acid (**9**). Then, reaction of (**9**) with acryloyl chloride gave the acrylate (**10**). In a third step,

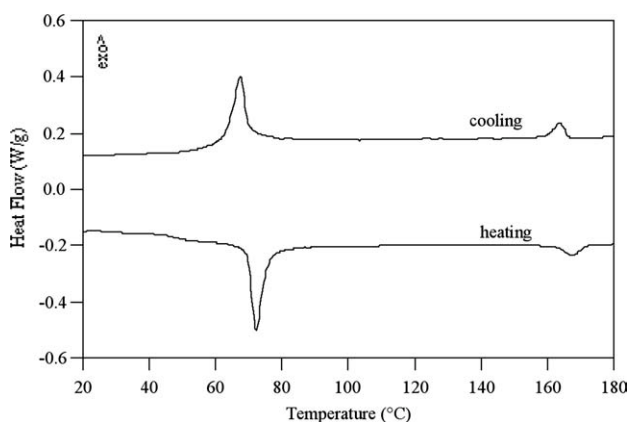


FIGURE 1 DSC traces of polymer p(1–8) (scan rate 10 °C/min).

esterification of (10) with 3-(perfluorooctyl)-1-propanol (2–8) in the presence of DCC and PPy led to the desired 3-(perfluorooctyl)-1-propyl 4-(3-acryloyloxypropyl-1-oxy)benzoate (1–8) monomer.

The fluorinated alcohols (2–6) and (2–8) used in the synthesis are not commercially available compounds and were prepared⁴⁴ via the regioselective, azobis(isobutyronitrile)-(AIBN)-initiated radical addition of the perfluoroalkyl iodide of selection to the double bond of allyl alcohol and subsequent reduction of the fluorinated iodoalcohol intermediate. These perfluoroalkylpropyl precursors were designed and preferred to the most common perfluoroalkylethyl precursors for incorporation into anisometric aromatic units, since the longer aliphatic segment was expected to enhance intramolecular phase segregation of the side chain core of the acrylate monomer, thereby increasing its mesogenic character. A trimethylene spacer segment was also used to connect the side chain to the acrylate moiety of the monomer, and eventually to the acrylate backbone of the derived polymer, to introduce sufficient conformational freedom enabling an ordered assembly of the side groups in a mesophase structure at accessible temperatures.

The polymerization reactions of the acrylate monomers, (1–6) and (1–8), to the respective polyacrylates, p(1–6) and p(1–8), were performed with free radical initiation (AIBN, 60 °C) in benzene solution (yields 70–85%). Both polymers were insoluble in common organic solvents, but soluble in fluorinated solvents such as trifluorotoluene and 1,1,2-trichlorotrifluoroethane, and their mixtures with chloroform. Because of this, molar mass and dispersity of the polymers could not be fully characterized by size exclusion chromatography. A weight average molar mass M_w of 70,000 g/mol was evaluated by light scattering measurements for p(1–6) only. Similar values of M_w were previously found for other perfluoroalkyl polyacrylates,⁴⁵ which confirms that such fluorinated acrylates can be conveniently free-radically polymerized to relatively high polymers.

Mesophase Behavior of the Polymers

Polarizing optical microscopy observations revealed the formation of a birefringent melt for both p(1–6) and p(1–8)

that cleared upon further heating to the isotropization temperature T_i . However, no specific optical textures were noted that could help identify the nature of the mesophases. The viscosity of the high molar mass polymers prevented the development of the textures associated with the various mesophases.

The phase transition temperatures, with relevant enthalpies, of the polymers were determined by differential scanning calorimetry (DSC) measurements or by wide-angle X-ray diffraction (WAXD) investigations. Above the glass transition temperature T_g , both polymers exhibited at least two phase transitions (Fig. 1), suggesting the occurrence of a polymorphic behavior (Table 1). In particular, p(1–6) formed a sequence of two mesophases between 17 °C (T_g) and 127 °C (T_i); p(1–8) gave rise to three successive mesophases between 48 °C (T_g) and 166 °C (T_i). Furthermore, a mesophase occurred at room temperature, above T_g , in p(1–6), whereas it was frozen in a glassy state, below T_g , in p(1–8). The increase in T_g in the latter polymer is consistent with the reduced flexibility of the polyacrylate main chain imposed by incorporation of the longer, rigid rod-like perfluoroalkyl chain in the side group. The higher aspect ratio of the fluorinated mesogenic unit in the side chain also accounts for the broader mesophase range with a higher T_i in p(1–8). The onset of different mesophases with decreasing degree of order with rising temperature was demonstrated by our investigations by X-ray diffraction. No mesophase was formed in either monomer 1–6 or 1–8. Thus, liquid crystallinity was stabilized in polymers only, where the anisometric side groups were interconnected along the polymer backbone.

X-Ray Diffraction Studies

To identify the mesophases, X-ray diffraction patterns of the two polymers were recorded on powder samples as a function of temperature. The structural parameters for the encountered mesophases are reported in Table 2. For p(1–8), the lower temperature diagrams showed one sharp wide-angle reflection pointing to the presence of a structure of the hexatic type with a pseudo-hexagonal lattice of side $a_H = 5.7 \text{ \AA}$ and an available average surface (S) per fluorinated side chain of $\sim 28 \text{ \AA}^2$ (Fig. 2, left). Three low-angle Bragg reflections with periodicities in the ratio 1:3:4 indicated a smectic (Sm) mesophase with an interlayer spacing $d = 49.8 \text{ \AA}$. Comparison of the measured d with the calculated length L ($L = 55 \text{ \AA}$) of a structural motif consisting of two antiparallel side groups pointing to opposite directions above and below the polyacrylate main chain^{46,47} suggests the side groups to be arranged in a double layer structure, either

TABLE 1 Transition Temperatures (in °C) (Enthalpies in J/g)^a for Polymers p(1–6) and p(1–8)

Polymer	Transition Temperature (Enthalpy)
p(1–6)	g 17 SmF ₂ (or SmI ₂) 113 (1.1) SmC ₂ 127 (0.7) iso
p(1–8)	g 48 SmI ₂ 74 (8.4) SmF ₂ 95 (nd) ^b SmC ₂ 166 (0.7) iso

^a By DSC, 10 °C/min heating rate. g: glassy; SmI₂, SmF₂, and SmC₂: double layer SmI, SmF, and SmC; iso: isotropic liquid.

^b Not detected; recorded by WAXD only.

TABLE 2 Structural Parameters of the Different Smectic Mesophases of Polymers p(1–6) and p(1–8)

Mesophase	Parameter	p(1–6)	p(1–8)
	L (± 1 Å)	50	55
SmI ₂	d (± 0.3 Å)		49.8
	a_H (± 0.1 Å)		5.7
	ϕ ($\pm 1^\circ$)		24
SmF ₂ ^a	d (± 0.3 Å)	41.7	48.1
	a_H (± 0.1 Å)	5.7	5.7
	ϕ ($\pm 1^\circ$)	33	28
SmC ₂	d (± 0.3 Å)	38.7	44.2
	D (± 0.1 Å)	5.1	5.0
	ϕ ($\pm 1^\circ$)	39	36

^a SmF₂ or SmI₂ for p(1–6).

tilted or interdigitated (Fig. 3). However, the terminal CF₃ groups are rather bulky with a van der Waals volume of the equivalent hemisphere of 42.6 Å³ (compare with 16.8 Å³ for the CH₃ group)^{48,49} and a large cross-section area of ~ 23 Å² as estimated by molecular models. For the given S , there would be an excessive steric hindrance for two antiparallel fluorinated tails to overlap within the layer of an interdigitated smectic phase, particularly in densely crowded polymers such as poly(acrylate)s. By contrast, an efficient space filling can be achieved by tilting the fluorinated side chains in an end-to-end arrangement of a double layer smectic structure. A maximum tilt angle ϕ of the mesogen long axis to the smectic plane normal of 24° was evaluated (Fig. 3). It is not known whether the mesogens had a synclinal or anticlinal correlation along the normal to the smectic planes.

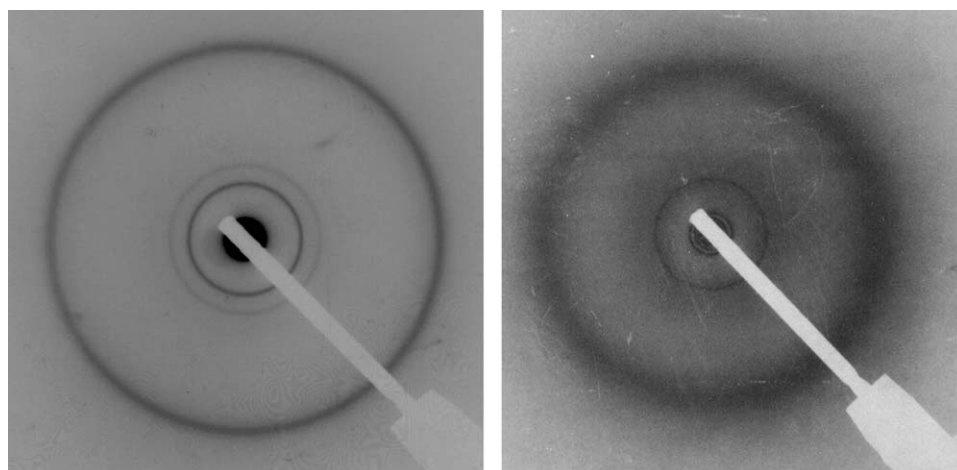
A variation in the diffraction pattern was revealed by heating the sample up to 95 °C with the appearance of two reflections in the low-angle region with a periodicity ratio 1:3 ($d = 48.1$ Å) and a wide angle reflection indicative of a pseudohexagonal lattice ($a_H = 5.7$ Å, $S \sim 28$ Å²). The comparison of d with L evidenced that the side chains were organized in a tilted, double layer structure with $\phi = 28^\circ$.

The diffraction patterns of the two high-order smectic phases are consistent with the presence of SmI₂ and SmF₂ mesophases. In both cases, the mesogens are organized over a pseudohexagonal lattice, but tilted toward the apex and the side of the hexagon in the SmI and SmF, respectively. There is a greater in-plane correlation length in the SmI than in the SmF phase.⁵⁰ However, the subtle differences in the tilt direction of the molecules in the two mesophases make it very difficult to recognize them, unless they are formed successively in a polymorphic polymer.⁵¹ In p(1–8) the phase transition SmI-SmF was associated with a decreased in-plane correlation and a shortened layer spacing.

Another significant modification of the X-ray diffraction pattern was observed above 95 °C (Fig. 2 right). The low-angle reflections, with a periodicity ratio of 1:3, indicated $d = 44.2$ Å corresponding to $\phi = 36^\circ$. A wide-angle diffuse halo was due to a mesophase lacking long-range in-plane correlation between the side chains (average intermolecular distance $D \sim 5.0$ Å, $S \sim 25$ Å²), such as in a SmC₂ phase.

p(1–6) exhibited temperature-dependent X-ray diagrams similar to those of the two higher temperature mesophases of p(1–8). Accordingly, a SmF₂ (or SmI₂) mesophase occurred at temperatures lower than 100 °C and a SmC₂ mesophase between 100 °C and the clearing temperature (Table 2).

For both polymers, d decreased, and apparently ϕ increased, in passing from the high-order smectic mesophase to the low-order smectic mesophase. Although this particular feature has already been noted for fluorinated polyacrylates,⁴⁵ it is actually rather uncommon for liquid crystals, in which normally either less tilted or orthogonal mesophases are originated at higher temperatures above tilted mesophases, the most frequent and best known of such phase transitions being the SmC-SmA transition with rising temperature. Shortening of d was due to a small shrinkage of the smectic layers probably because of conformational changes in the perfluorinated chain groups and/or the spacer segments at the higher temperatures. The layer thickness remained constant all over the range of existence of each smectic

**FIGURE 2** X-ray diffraction patterns of p(1–8) at 65 °C (left) and at 160 °C (right).

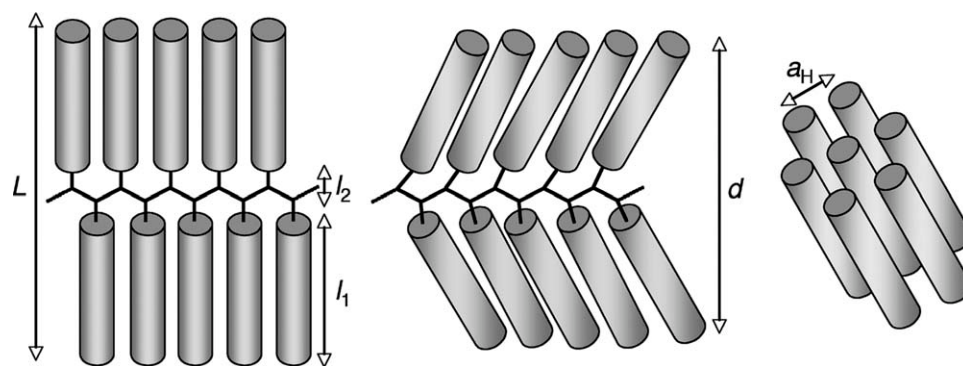


FIGURE 3 Schematic of a double layer, tilted smectic mesophase with pseudo-hexagonal packing of mesogens.

mesophase, a decrease in d being detected at the phase transition temperatures only. Examples of polymorphism in the liquid crystalline state of fluorinated polymers are rare in the literature.^{35,45,52}

Electron Density Profiles

It was not possible to draw oriented fibers of the polymers from their mesophase states, and the nature of the tilted mesophase could not be confirmed on well-aligned specimens. Further support to the formation of tilted mesophases was provided by an evaluation of the electron density profiles $\rho(z)$ along the layer normal of the smectic mesophases.⁴⁰

As one example we discuss the electron density profiles derived from the intensities of the low-angle reflections in the smectic I mesophase of p(1–8). Analogous considerations apply to the other mesophases of both polymers. There were

three reflection orders of amplitude $a_1 = 1.00$, $a_3 = 0.32$, and $a_4 = 0.15$ ($a_2 = 0$), which resulted in eight density profiles. Only four density profiles (combinations of signs ρ_{-+-} , ρ_{-++} , ρ_{--+} , and ρ_{---}) are shown in Figure 4, the four symmetrical ones being omitted for brevity.

The $\rho(z)$ profiles (e)–(h) (not shown) exhibited a central minimum for the fluorinated chains ($\sim 0.3 < z/d < \sim 0.7$), for which by contrast the expected electron density (ρ_0) was maximum ($\rho_0 = 16 \text{ e}/\text{\AA}$). The profiles (c) and (d) were also discarded because they showed two minima for the polymer main chains ($z/d = 0$ and 1), for which $\rho_0 = 9 \text{ e}/\text{\AA}$ was calculated. The last two profiles (a) and (b) appeared to be both physically acceptable, but (b) (sign combination ρ_{-++}) was preferred as it showed two minima corresponding to the methylene spacers ($z/d \sim 0.1$ and 0.9 ; $\rho_0 = 6 \text{ e}/\text{\AA}$), besides an absolute maximum for the fluorinated tails and

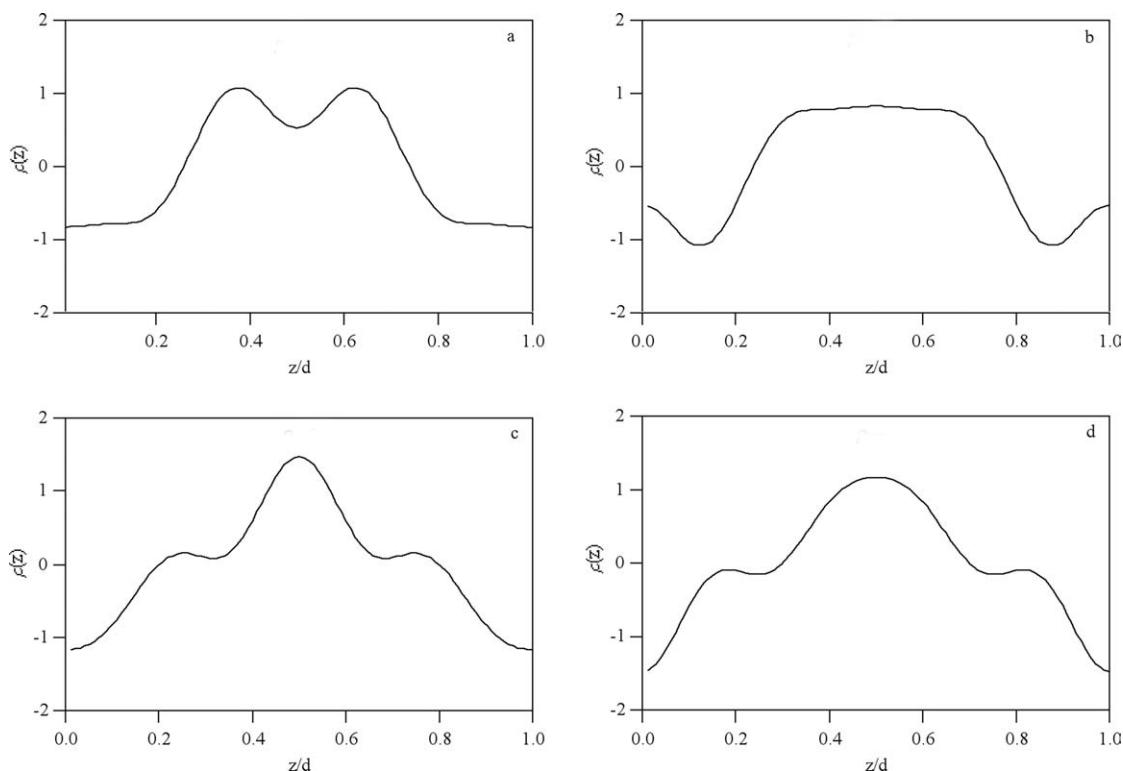


FIGURE 4 Electron density profiles for the smectic I phase of p(1–8), at room temperature on cooling from the isotropic melt, for combinations of signs: (a) ρ_{-+-} , (b) ρ_{-++} , (c) ρ_{+--} , and (d) ρ_{---} . The four symmetrical profiles are not shown.

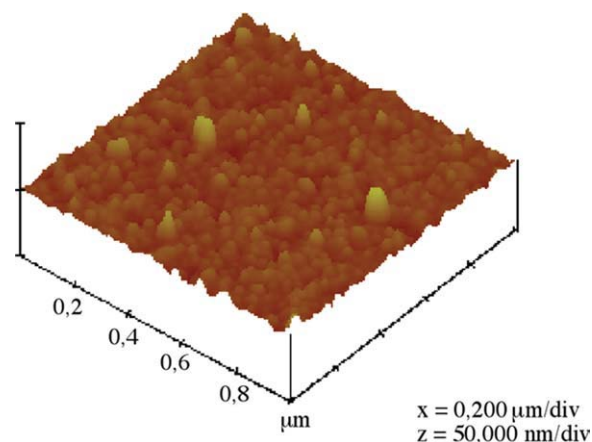


FIGURE 5 TM-AFM imaging of a polymer film of p(1–8).

secondary, comparatively weak maxima corresponding to the hydrocarbon main chains. Furthermore, the central maximum in $\rho(z)$ was not sufficiently intense to account for interdigitation of two, even partly, overlapping fluorinated chains. Therefore, the side mesogenic groups were arranged in a double layer, tilted smectic mesophase for which ϕ could be estimated (Table 2).

Wettability Studies

To evaluate the effect of surface structure and ordering on surface energy, contact angles θ of the polymer films were measured using a range of *n*-alkanes (C7, C8, C10, C12, and C16) as apolar liquids and water as polar liquid. Prior to measurements, the cast and thermally annealed films were analyzed by tapping-mode atomic force microscopy (TM-AFM). The film surfaces were relatively smooth (RMS < ~100 nm) and displayed no regular ordered topographies (Fig. 5). This made it possible to compare the values of θ found with the different solvents.

The values of θ with water and *n*-hexadecane are conventionally used to estimate qualitatively hydrophobicity ($\theta_w > \sim 90^\circ$) and lipophobicity ($\theta_{hd} > \sim 60^\circ$), respectively. The fluorinated polyacrylates showed large contact angles with all the interrogating liquids, exhibiting distinct hydrophobic ($\theta_w \geq 105^\circ$) and lipophobic ($\theta_{hd} \geq 74^\circ$) properties (Table 3). This twofold character is typical of fluorinated polymers, as opposed to most other polymers that are hydrophobic, but not lipophobic at the same time.

For both p(1–6) and p(1–8) films a continuous increase in contact angle was detected with increasing surface tension

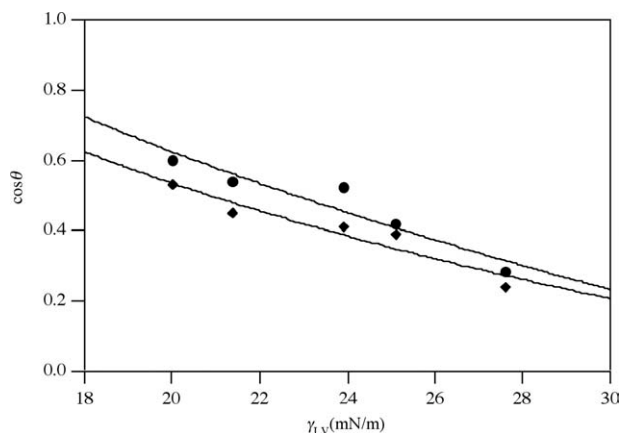


FIGURE 6 $\cos\theta$ versus γ_{LV} trends for p(1–6) (●) and p(1–8) (◆) with best fit of the Li–Neumann equation of state ($\beta = 3.211 \times 10^{-4} \text{ (m/mN)}^2$ for p(1–6) and $\beta = 1.450 \times 10^{-4} \text{ (m/mN)}^2$ for p(1–8)).

γ_{LV} of the *n*-alkanes. One can also note that the contact angle values depended on the length of the perfluorinated tail incorporated in the side chain, the values of θ being higher for the perfluorooctyl containing films.

It is common practice in surface science to use contact angles data for the evaluation of solid surface tension. However, the correlation between θ and γ_S is still a controversial question and none of the various methods proposed are generally accepted.^{53,54} Therefore, we followed two conceptually different approaches to evaluating γ_S from θ , namely an additive component approach and an equation-of-state approach.

The former method was after Owens, Wendt, and Kaelble (OWK)^{41,42} that relies on the Fowkes's model⁵⁵ assuming the total surface energy to be the sum of different interaction components (van der Waals dispersive, dipole, hydrogen bonding, etc.) at the liquid–solid interface and postulating a geometric mean relationship for both of the solid–liquid and liquid–liquid interfacial tensions. γ_S is computed as the sum of dispersion and polar components, γ_S^d and γ_S^p , respectively (eq 2). The latter method followed the equation of state of Li and Neumann (LN) (eq 4).⁴³ This is essentially based on a modification of the Berthelot's combining rule,⁵⁶ that states the potential energy parameter of unlike-pair molecular interactions to be the geometric mean of the potential energy parameters of like-pair molecular interactions. The LN approach provides γ_S by fitting the $\cos\theta$ values found with a set of probing liquids of varied surface tension γ_{LV}

TABLE 3 Contact Angles θ^a and Solid-Surface Tension γ_S for Polymers p(1–6) and p(1–8)

Polymer	θ_w (°)	θ_h (°)	θ_o (°)	θ_d (°)	θ_{dd} (°)	θ_{hd} (°)	γ_S^{db} (mN/m)	γ_S^{pb} (mN/m)	γ_S^{OWKb} (mN/m)	γ_S^{LNc} (mN/m)
p(1–6)	105	53	57	59	65	74	12.7	2.0	14.7	13.5
p(1–8)	113	58	63	66	67	76	11.5	0.8	12.3	12.0

^a Measured with water, *n*-heptane, *n*-octane, *n*-decane, *n*-dodecane, and *n*-hexadecane.

^b Calculated with the Owens–Wendt–Kaelble method: γ_S^d dispersion component, γ_S^p polar component.

^c Calculated with the Li–Neumann method.

(Fig. 6). Values of the constant β narrowly scattered around the average value of $1.234 \times 10^{-4} \text{ (m/mN)}^2$ have been reported in the literature.⁵⁴

The values of γ_s calculated by the two independent approaches agreed quite well with each other, demonstrating a low surface energy of the polymer films (Table 3). The dispersive component overwhelmed the associated polar component γ_s^p in determining the total surface tension, as the fluorinated surfaces experienced dispersion forces but prevented polar interactions. Both γ_s^d and γ_s^p were lower for p(1-8) than for p(1-6). The longer perfluorooctyl chains induce a more effective surface segregation at the air-polymer interface, which would account for the lower values of surface energy.

Surface micro- and nanophase segregation is a specially relevant phenomenon in thin films of fluorinated polymers. Preferential migration to the outermost surface in fact occurs to minimize the surface and interface energies of the system and gives rise to enrichment of fluorine atoms in the surface phase with respect to the depleted bulk phase.⁵⁷ Gradient chemical structures have been proven by element sensitive depth profiling, for example, by X-ray photoelectron spectroscopy (XPS) and near-edge X-ray fine absorption structure spectroscopy (NEXAFS); for very recent investigations see.^{58,59} Furthermore, the often contrasting tendencies for liquid crystalline polymers to mesophase ordering and to structure and morphology formation result in assemblies with order and orientation at different length scales from the bulk to the surface of the films.^{35,60} Polymers carrying perfluoroalkylethyl side groups have been shown to self-organize in liquid crystalline surface structures, where the rodlike perfluorinated chains were stretched outwards at the polymer-air interface.^{5,61} The NEXAFS orientational order parameter increased with length of the perfluoroalkyl segments (from 4 to 8 CF₂ groups). In general, the surface had a higher degree of order than the bulk, independent of the bulk phase, and a liquid crystalline bulk phase caused a higher surface order than an isotropic bulk phase. More importantly for the sake of our discussion, a correlation was found between the increasing order parameter and the decreasing surface energy at room temperature.⁶¹ The segregation of the CF₃ terminal groups of the fluoroalkyl segment, which is responsible for the low surface energy,⁶² was enhanced by the orientation of the fluoroalkyl side chains.⁶³ Thus, the bulk phase appeared to ultimately determine the achievable surface order and the surface energy associated with it.⁶¹

The low wetting properties of the films of p(1-6) and p(1-8) derive from surface segregation of the perfluorinated tails, that can be enhanced by their anisotropic orientation in a liquid crystalline surface structure. The lower γ_s evaluated for p(1-8) is in agreement with the stronger mesogenic character of the longer perfluorooctyl chain and its better orientation. We propose that the high order of the bulk mesophase, for example the close-packed, pseudo-hexagonal SmI₂ mesophase of p(1-8), is sustained at the surface mesophase and favors lowering of the surface free energy. Note that the lowest value of γ_s reported in the literature is possibly that evaluated ($\gamma_s = 6.7 \text{ mN/m}$) for epitaxially grown crystallites of *n*-perfluoro-

cosane (C₂₀F₄₂) with an hexagonal closed array of CF₃ groups on the surface.⁶² Liquid-crystalline surface structures are also considered more stable to surface reconstruction upon ageing in different conditions than amorphous surface structures.^{4,9} The introduction of a mesogenic core, such as the perfluoroalkyl benzoate core, contributes to the organization and stabilization of the fluorinated chains at the surface of the films of p(1-6) and p(1-8).

CONCLUSIONS

New polyacrylates carrying a spaced perfluoroalkylpropyl benzoate side group of different length (6 and 8 CF₂ groups) were synthesized. Although relatively long perfluoroalkyl chains are *per se* mesogenic components of liquid crystalline polymers, their tendency to mesophase formation was greatly reinforced when linked to the phenyl ring of a benzoate core. The nature and polymorphism of the mesophases depended on the length of the perfluoroalkyl chain and changed from high-order to low-order structures with increasing temperature up to isotropization.

The existence of a mesophase at room temperature was related with the occurrence of both hydrophobic and lipophobic properties. The low wettability of fluorinated polymer surfaces is generally due to the surface segregation of the low surface tension fluorinated moieties. However, it may be further diminished by orientation and order of the fluoroalkyl mesogens residing in a smectic mesophase at the polymer-air interface. We suggest the high molecular order of the bulk mesophase to be transferred to the surface mesophase. A correlation between bulk order and surface order has been proposed for poly(perfluoroalkyl methacrylate)s,⁶¹ but basically nothing is known for fluorinated polymers where more complex, polymorphic structures exist. Conformational freedom introduced by flexible segments spacing the mesogenic core from the polymer backbone is another parameter that can govern mesophase structure and degree of order of the polymers.

The nonpolar and ordered nature of perfluoroalkyl liquid crystalline surfaces makes them potentially useful in a wide range of technological applications of inert, nonwetting films from photonics and optoelectronics to medicine and biology. We are interested in thin films for alignment layers of ferroelectric/antiferroelectric liquid crystals in electrooptical devices⁶⁴ and for nonbiocidal, nontoxic coatings with antibiofouling performance in the marine and freshwater environments.⁶⁵

The work was funded by the EU Framework 6 Integrated Project 'AMBIO' (Advanced Nanostructured Surfaces for the Control of Biofouling) and the Italian MiUR (fondi PRIN).

REFERENCES AND NOTES

- Volkov, V. V.; Platé, N. A.; Takahara, A.; Kajiyama, T.; Amaya, M.; Murata, Y. *Polymer* 1992, 33, 1316.
- Percec, V.; Lee, M. J. *Macromol Sci Pure Appl Chem* 1992, A29, 723.

- 3** Krupers, M.; Möller, M. *Macromol Chem Phys* 1997, 198, 2163.
- 4** Xiang, M.; Li, X.; Ober, C. K.; Char, K.; Genzer, J.; Sivaniyah, E.; Kramer, E. J.; Fischer, D. A. *Macromolecules* 2000, 33, 6106.
- 5** Li, X.; Andruzzi, L.; Chiellini, E.; Galli, G.; Ober, C. K.; Hexemer, A.; Kramer, E. J.; Fischer, D. A. *Macromolecules* 2002, 35, 8078.
- 6** Hartmann, P. C.; Collet, A.; Viguier, M.; Blanc C. *J Fluorine Chem* 2004, 125, 1909.
- 7** Ragnoli, M.; Pucci, E.; Bertolucci, M.; Gallot, B.; Galli, G. *J Fluorine Chem* 2004, 125, 283.
- 8** Martinelli, E.; Glisenti, A.; Gallot, B.; Galli, G. *Macromol Chem Phys* 2009, 210, 1746.
- 9** Caillier, L.; Taffin de Givenchy, E.; Geribaldi, S.; Guittard, F. *J Mater Chem* 2008, 18, 5382.
- 10** Mahler, W.; Guillon, D.; Skoulios, A. *Mol Cryst Liq Cryst* 1985, 2, 111.
- 11** Viney, C.; Twieg, R. J.; Russel, T. P.; Depero, L. E. *Liq Cryst* 1989, 5, 1783.
- 12** Viney, C.; Twieg, R. J.; Gordon, B. R.; Rabolt, J. F. *Mol Cryst Liq Cryst* 1991, 198, 285.
- 13** Wilson, L. M. *Macromolecules* 1995, 28, 325.
- 14** Napoli, M. *J Fluorine Chem* 1996, 79, 59.
- 15** Semenov, A. M.; Vasilenko, S. V. *Sov Phys JEPT* 1986, 63, 70.
- 16** Bunn, C. W.; Howells, E. R. *Nature* 1954, 174, 549.
- 17** Russell, T. P.; Rabolt, J. F.; Twieg, R. J.; Siemens, R. L.; Farner, B. L. *Macromolecules* 1986, 19, 1135.
- 18** Ropers, M. H.; Stébé, M. J.; Schmitt, V. *J Phys Chem B* 1999, 103, 3468.
- 19** Lester, C. L.; Guymon, A. C. *Macromolecules* 2000, 33, 5448.
- 20** Johansson, G.; Percec, V.; Ungar, G.; Smith, K. *Chem Mater* 1997, 9, 164.
- 21** Percec, V.; Schlueter, D.; Kwon, Y. K.; Blackwell, J.; Moeller, M.; Slangen P. J. *Macromolecules* 1995, 28, 8807.
- 22** Johansson, G.; Percec, V.; Ungar, G.; Zhou J. P. *Macromolecules* 1996, 29, 646.
- 23** Wang, J.; Ober, C. K. *Macromolecules* 1997, 30, 7560.
- 24** Beyou, E.; Babin, P.; Bennetau, B.; Dunogues, J.; Teyssie, D.; Boileau, S. *J Polym Sci Part A: Polym Chem* 1994, 32, 1673.
- 25** Bracon, F.; Guittard, F.; Taffin de Givenchy, E.; Cambon, A. *J Polym Sci Part A: Polym Chem* 1999, 37, 4487.
- 26** Hudson, S. D.; Jung, H. T.; Percec, V.; Cho, W. D.; Johansson, G.; Ungar, G.; Balagurusamy, V. S. K. *Science* 1997, 278, 449.
- 27** Percec, V.; Glodde, M.; Bera, T. K.; Miura, Y.; Shiyanovskaya, I.; Singer, K. D.; Balagurusamy, V. S. K.; Heiney, P. A.; Schnell, I.; Rapp, A.; Spiess, H. W.; Hudson, S. D.; Duan, H. *Nature* 2002, 419, 384.
- 28** Percec, V.; Imam, M. R.; Bera, T. K.; Balagurusamy, V. S. K.; Peterca, M.; Heiney, P. A. *Angew Chem Int Ed* 2005, 44, 4739.
- 29** Nguyen, H. T.; Sigaud, G.; Achard, M. F.; Hardouin, F. T.; Twieg, K.; Betterton, R. *Liq Cryst* 1991, 10, 389.
- 30** Liu, H.; Nohira, H. *Liq Cryst* 1997, 22, 217.
- 31** Chen, B. Q.; Yang, Y. G.; Wen, J. X. *Liq Cryst* 1998, 24, 539.
- 32** Taffin de Givenchy, E.; Guittard, F.; Bracon, F.; Cambon, A. *Liq Cryst* 1999, 26, 1371.
- 33** Guittard, F.; Taffin de Givenchy, E.; Geribaldi, S.; Cambon, A. *J Fluorine Chem* 1999, 100, 85.
- 34** Muthukumar, M.; Ober, C. K.; Thomas, E. L. *Science* 1997, 277, 1225.
- 35** Al-Hussein, M.; Séréro, Y.; Konovalov, O.; Mourran, A.; Möller, M.; de Jeu, W. H. *Macromolecules* 2005, 38, 9610.
- 36** Hikita, M.; Tanaka, K.; Nakamura, T.; Kajiyama, T.; Takahara, A. *Langmuir* 2004, 20, 5304.
- 37** Wang, J.; Mao, G.; Ober, C. K.; Kramer, E. J. *Macromolecules* 1997, 30, 1906.
- 38** Davidson, T.; Griffin, A. C.; Wilson, L. M.; Windle, A. H. *Macromolecules* 1995, 28, 354.
- 39** Gudkov, V. A.; *Kristallogr* 1984, 29, 529; *ibidem* 1984, 29, 1122.
- 40** Davidson, P.; Levelut, A. M.; Achard, M. F.; Hardouin, F. *Liq Cryst* 1989, 4, 561.
- 41** Owens, D. K.; Wendt, R. C. *J Appl Polym Sci* 1969, 13, 1741.
- 42** Kaelble, D. H. *J Adhesion* 1970, 2, 66.
- 43** Li, D.; Neumann, A. W. *J Colloid Interf Sci* 1992, 148, 190.
- 44** Ren, Y.; Lodge, T. P.; Hillmyer, M. A. *Macromolecules* 2001, 34, 4780.
- 45** Andruzzi, L.; D'Apollo, F.; Galli, G.; Gallot, B. *Macromolecules* 2001, 34, 7707.
- 46** Honda, K.; Morita, M.; Otsuka, H.; Takahara, A. *Macromolecules* 2005, 38, 5699.
- 47** de Crevoisier, G.; Fabre, P.; Leibler, L.; Tencé-Girault, S.; Corpart, J. M. *Macromolecules* 2002, 35, 3880.
- 48** Seebach, D. *Angew Chem Int Ed Engl* 1990, 29, 1320.
- 49** Bondi, A. *J Phys Chem* 1964, 68, 441.
- 50** Gane, P. A. C.; Leadbetter, A. J.; Benattar, J. J.; Moussa, F.; Lambert, N. *Phys Rev A* 1981, 24, 2694.
- 51** Gallot, B.; Galli, G.; Ceccanti, A.; Chiellini, E. *Polymer* 1999, 40, 2561.
- 52** Galli, G.; Martinelli, E.; Chiellini, E.; Ober, C. K.; Glisenti, A. *Mol Cryst Liq Cryst* 2005, 441, 211.
- 53** Della Volpe, C.; Maniglio, D.; Brugnara, M.; Siboni, S.; Morra, M. *J Colloid Interf Sci* 2004, 271, 434.
- 54** Kwok, D. Y.; Neumann, A. W. *Adv Colloid Interf Sci* 1999, 81, 167.
- 55** Fowkes, F. M. *Ind Eng Chem* 1964, 56, 40.
- 56** Berthelot, D.; *Compt Rend* 1898, 126, 1857.

- 57** Thomas, R. R.; Anton, D. R.; Graham, W. F.; Darmon, M. J.; Sauer, B. B.; Stika, K. M.; Swartzfager, D. G. *Macromolecules* 1997, 30, 2883.
- 58** Mielczarski, J.; Mielczarski, E.; Galli, G.; Morelli, A.; Martinelli, E.; Chiellini, E. *Langmuir* 2010, 26, 2871.
- 59** Sohn, K. E.; Dimitriou, M. D.; Genzer, J.; Fischer, D. A.; Hawker, C. J.; Kramer, E. J. *Langmuir* 2009, 25, 6341.
- 60** Busch, P.; Krishnan, S.; Paik, M.; Toombes, G. E. S.; Smilgies, D.-M.; Gruner, S. M.; Ober, C. K. *Macromolecules* 2007, 40, 81.
- 61** Lüning, J.; Stöhr, J.; Song, K. Y.; Hawker, C. J.; Iodice, P.; Nguyen, C. V.; Yoon, D. Y. *Macromolecules* 2001, 34, 1128.
- 62** Nishino, T.; Meguro, M.; Nakamae, K.; Matsushita, M.; Ueda, Y. *Langmuir* 1999, 15, 4321.
- 63** Nishino, T.; Urushihara, Y.; Meguro, M.; Nakamae, K. *J Colloid Interf Sci* 2005, 283, 533.
- 64** Bennis, N.; Spadlo, A.; Dabrowski, R.; Martinelli, E.; Galli, G.; Quintana, X.; Oton, J. M.; Geday, M. A. *Opto-Electron Rev* 2006, 14, 281.
- 65** Marabotti, I.; Morelli, A.; Orsini, L. M.; Martinelli, E.; Galli, G.; Chiellini, E.; Lien, E. M.; Pettitt, M. E.; Callow, M. E.; Callow, J. A.; Conlan, S. L.; Mutton, R. J.; Clare, A. S.; Kocijan, A.; Donik, C.; Jenko, M. *Biofouling* 2009, 25, 481.